THE ASTROPHYSICAL JOURNAL, 421:L31–L34, 1994 January 20

THE DYNAMICAL AND RADIATIVE EVOLUTION OF CLUMPY SUPERNOVA EJECTA

M. C. ANDERSON, T. W. JONES, AND L. RUDNICK
Astronomy Department, University of Minnesota, Minneapolis, MN 55455
I. L. TREGILLIS
School of Physics and Astronomy, University of Minnesota, Minneapolis, MN 55455
AND
HYESUNG KANG
Department of Earth Sciences, Pusan National University, Pusan 609-735, Korea
Received 1993 September 10; accepted 1993 November 1

ABSTRACT

Numerical simulations describing the dynamical and radiative evolution of clumpy supernova ejecta are compared with observations of optical and radio emission knots in SNR Cassiopeia A. Three major phases are identified in the evolution of clumpy ejecta: a bow-shock phase, an instability phase, and a dispersal phase. The phenomenological and radiative signatures of each phase are discussed and compared with multiepoch measurements of small-scale features in Cas A. Good correspondence is found between theory and observations. Both support the premise that compact radio emission features are controlled more by magnetic field amplification triggered in the instability phase than by in situ acceleration of new relativistic particles.

Subject headings: acceleration of particles — shock waves — supernova remnants

1. INTRODUCTION

Until recently, supernovae have typically been modeled as smooth, continuous distributions of stellar material. High-resolution observations of young supernova remnants (SNRs), however, now suggest that these sources may be better described in terms of both smooth and clumpy ejecta components. Small-scale brightness irregularities in radio, optical and X-ray images of young historical remnants (e.g., Cas A, Tycho's and Kepler's SNRs) suggest underlying condensations exist in the emitting material. Several remnants exhibit fast-moving knots of chemically enriched materials. Clumping of ejecta has been invoked to explain several large-scale mixing-related phenomena observed in SN 1987A (see Hachisu et al. 1990 for a summary). This clumpy component must be reckoned with in discussing the dynamical and radiative evolution of young SNRs.

The condensation of clumpy ejecta is believed to stem from an early epoch of dynamical instability, occurring while the blast wave is still inside the progenitor star (Chevalier & Klein 1978; Müller & Arnett 1982). Upon passage of the blast wave, the interface between the mantle and the stellar envelope is found to be Rayleigh-Taylor (R-T) unstable—Jones, Smith, & Straka (1981) speculate that R-T fingers may decouple as clumps from the surrounding outflow at this time. Eventually these clumps may ablate completely and meld with the diffuse ejecta (Hamilton 1985).

In this *Letter* we will take a closer look at the dynamical and radiative evolution of individual ejecta clumps. We focus on the young, well-studied SNR Cassiopeia A, which exhibits knots of both optical and radio emission. The enriched composition and high Doppler velocities (~ 6000 km s^{-1}) evident in the spectra of the fast-moving optical knots (FMKs) in Cas A (van den Bergh 1971) suggest that these knots are comprised of material ejected from the core of a massive star. An explosion date of 1658 ± 3 has been derived from the proper motions of 95 FMKs (van den Bergh & Kamper 1983). This is in good agreement with the likely historical observation by Flamsteed in 1680 (Ashworth 1980), implying that these clumps have not yet been significantly decelerated. Radio knots are often interpreted as sites of locally enhanced relativistic particle acceleration (see e.g., Bell 1977; Dickel & Greisen 1979; Cowsik & Sarkar 1984). Proper-motion studies show that these features are significantly decelerated, with expansion ages ~ 900 yr (Tuffs 1986; Anderson & Rudnick 1994a, hereafter ARI). There have been no confirmed cases of spatial coincidence between radio and optical knots.

The physical connection between these two systems of knots has not yet been well established. Are both radio and optical knots associated with a clumpy component of the ejecta, or are they more recently formed local enhancements in the underlying diffuse component? What physical factors cause each type to "turn on"? Why do knots not exhibit *both* radio *and* optical emission? Why do optical FMKs have such significantly shorter expansion timescales than radio knots? What regulates the radiative lifetimes of these features?

Good observational and theoretical progress has recently been made toward understanding the dynamical evolution of clumpy SNR ejecta. A recent multiepoch study of the proper motions, brightness evolution and synchrotron spectra of 304 compact radio features in Cas A has greatly clarified the nature of these features (ARI; Anderson & Rudnick 1994b, hereafter ARII). Recent numerical simulations of supersonic clumps and associated particle acceleration revealed an evolutionary cycle consistent with these observations (Jones, Kang, & Tregillis 1993, hereafter JKT). Here we tie these observations and simulations together to provide a comprehensive overview of the manner in which clumpy ejecta in young SNRs evolve, from both phenomenological and radiative viewpoints. The discussion also explores how new relativistic particles can be accelerated around an ejecta clump and the way clumps may influence the local magnetic field. These theoretical expectations are then compared with observations of SNR Cas A.

2. THE EVOLUTIONARY SEQUENCE FOR CLUMPY EJECTA

Numerical simulations tracing the time evolution of supersonic gaseous projectiles show three major dynamical phases (see Fig. 1 [Pl. L6]). In the initial "bow-shock phase" (Fig. 1 [*top*]), the clump drives a bow shock before it into the surrounding medium, while a secondary shock is transmitted into the clump itself. The clump begins to decelerate as a body when the internal shock reaches the rear of the clump, initiating R-T instabilities—this begins an "instability phase" (Fig. 1 [*middle*]). On a somewhat longer timescale, these instabilities shred the clump into a system of blobs and filaments—we label this the "dispersal phase" (Fig. 1 [*bottom*]).

The factor controlling the evolutionary rate through these three phases is the density contrast between the clump material and the ambient medium, given by $\chi = \rho_c/\rho_{amb}$, where ρ_c and ρ_{amb} are the clump and ambient densities, respectively. When $\chi \gg 1$, the three evolutionary phases outlined above will occur well before the nominal ram pressure "stopping time," usually defined as the timescale over which the clump intercepts its own mass from the ambient material. As long as the clump's motion is highly supersonic, its evolution is largely independent of Mach number. Below we examine these events in greater detail, focusing on the phenomenological and radiative signatures of each. We show how each phase may be reflected in various features observed in Cas A. JKT and ARI provide more detailed discussions of the theory and observations.

2.1. *The Bow-Shock Phase*

2.1.1. *Phenomenological Signature*

Once ejected, a clump forms several shocks (see Fig. 1 [*top*]), including a bow shock that compresses any swept-up magnetic field. Relativistic particles may be accelerated at the bow shock. A second shock (also apparent in Fig. 1 [*top*]), driven into the clump by the stagnation pressure on its nose, will traverse the clump on a timescale $t_{bc} \approx C(\chi)(\chi^{1/2}D/u_c)$, where D is the clump radius, u_c is the clump velocity, and $C(\chi) < 1$. Flow sweeping around the clump will be unstable to Kelvin-Helmholtz (K-H) instabilities, leading to the formation of a flocculent boundary layer. Some material is stripped from the clump as a consequence, but this development is not disruptive. Any magnetic field embedded in the boundary layer begins to be amplified by field-line stretching.

2.1.2. *Radiative Signature*

Total radio intensity.—Our simulations (JKT) indicate that these structures will be relatively faint in the radio (see Fig. 2 [*top*] [Pl. L7]), particularly in comparison with what develops later. However, if viewed against a low emissivity background, weak emission may be detectable from particles and fields compressed by bow shocks—the faint paraboloidal structures seen around the edges of the Cas A remnant may be such examples, as proposed by Braun, Gull, & Perley 1987, hereafter BGP). That these shocks can have very low surface brightness suggests that many bow shocks may remain undetected. It is therefore difficult to estimate the total volume filling factor of diffuse material in the remnant that has been processed by bow shocks, but it may be quite large. If there is a significant magnetic field initially in the clump boundary layer, its amplification may make the boundary layer competitive with the bow shock as a source of synchrotron emission, even during this phase.

Polarization.—True bow shocks may be distinguished from other emission features by a characteristic synchrotron polarization pattern, tangential to the bow-shaped profile. Tangential fields are observed in many of the features selected by BGP. In addition, arclike structures with tangential fields have been identified in maps of polarized intensity at $\lambda = 20$ cm (Anderson, Keohane, & Rudnick 1994). These arcs are quite faint in total intensity, in concordance with the simulations of JKT.

Spectral index.—The spectral index of bow-shock radio emission is determined by the clump dynamics, in particular by the Mach number of the bow shock. In the first-order Fermi, test particle limit, a Mach M shock in a $\gamma = 5/3$ gas yields an equilibrium synchrotron spectral index α (where $S_\nu \propto \nu^{-\alpha}$) given by $\alpha = (M^2 + 3)/2(M^2 - 1)$. As an example, BGP estimate $M = 2.3$ for the bow-shock feature they designate "C," based on the opening angle of the paraboloid. The above equation then predicts $\alpha = 0.97$—close to the observed value of 0.88 (ARII), especially since the observed Mach number is likely to be an underestimate of the true asymptotic opening angle, which is reached far from the region where radio emission is easily visible.

Optical.—It is generally assumed that the optical fast-moving knots in Cas A are clumps of ejecta dense enough that the internal shock becomes radiative on short timescales. The fact that FMKs remain undecelerated at the present epoch (van den Bergh 1971) attests to high internal densities—in ARI a characteristic FMK density contrast of $\chi \approx 100$ is suggested. Kamper & van den Bergh (1976) measure characteristic optical knot e-folding lifetimes of 25 yr. If we assume this brightness rise time corresponds roughly to the timescale for the internal shock to reach the core of the clump, then an optical lifetime of $\sim \frac{1}{2} t_{bc}$ is obtained. Van den Bergh (1971) quotes typical FMK diameter of 2″, so with $\chi \sim 100$ and $u_c = 6000$ km s^{-1}, optical knot lifetimes are expected to be ~ 20 yr—comparable to the observed lifetimes. Because optical knots are observed primarily in the vicinity of the bright radio ring, the faint radio emission from their bow shocks may be imperceptible.

2.2. *The Instability Phase*

2.2.1. *Phenomenological Signature*

The JKT models show that the initiation of deceleration (as the internal shock exits the rear of the clump on a timescale of order t_{bc}) is accompanied by the development, on this same timescale, of R-T fingers along the forward face of the clump (See Fig. 1 [*middle*]). Along with mixing induced by K-H instabilities in the clump boundary layer, these fingers stretch and amplify the local magnetic field. For supersonic clumps, magnetic field amplification may continue over several orders of magnitude until the field becomes dynamically important or until it is limited by other nonlinear processes such as reconnection (JKT).

2.2.2. *Radiative Signature*

Total radio intensity.—JKT show that clump deceleration may be accompanied by a rapid increase in synchrotron emissivity which is in many ways analogous to the radio turn-on predicted by Gull (1975) for the decelerating diffuse ejecta shell. JKT find that the synchrotron emission from the regions of amplified field in the shear layers surrounding the clump is much stronger than the emission from particles compressed and accelerated at the bow-shock. In their models, synchrotron turn-on occurs roughly exponentially, with timescales com-

PLATE L6

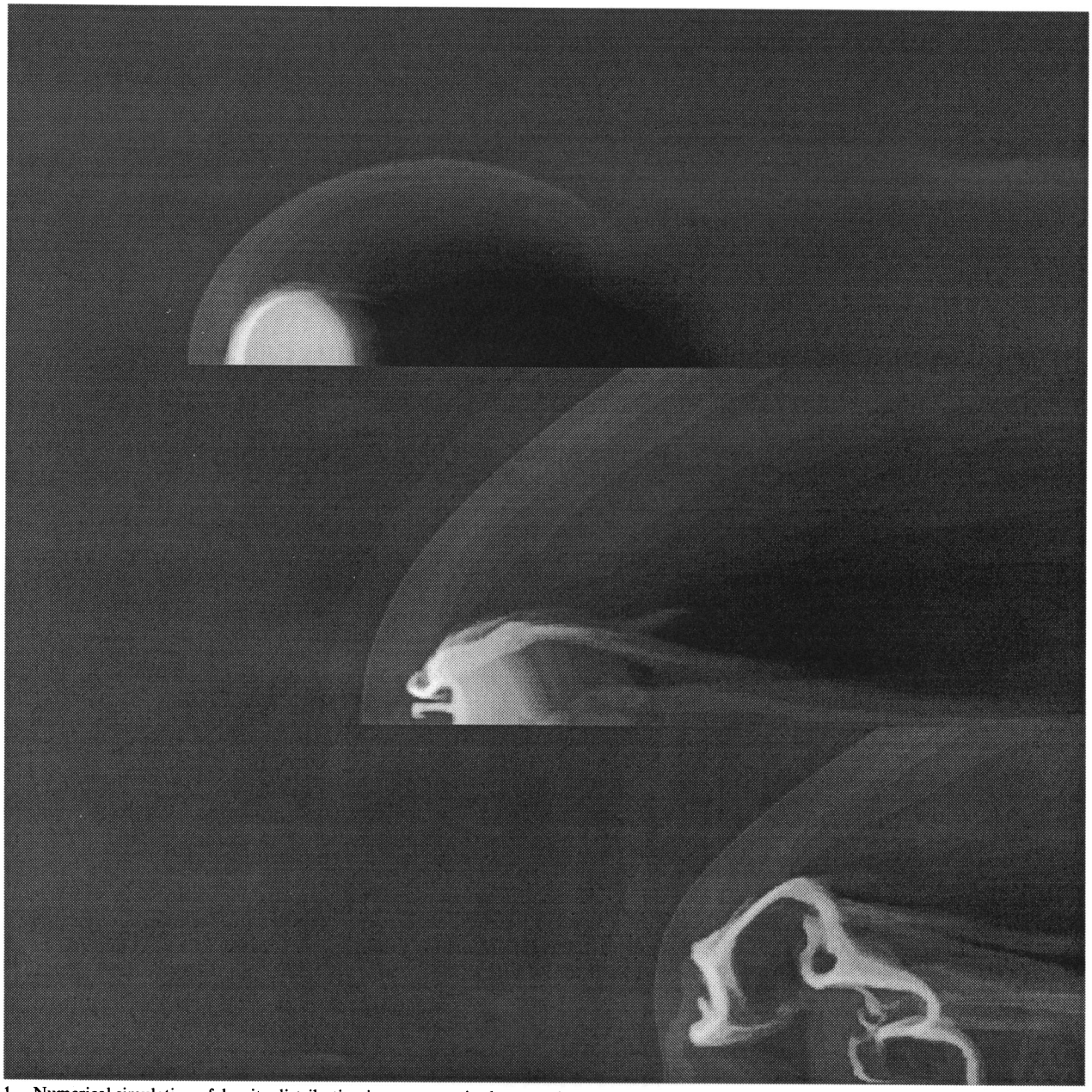

FIG. 1.—Numerical simulation of density distribution in a supersonic clump at three time steps characterizing the major phases of dynamical evolution: (*top*) the bow-shock phase, (*middle*) the instability phase, and (*bottom*) the dispersal phase. The clump began with a density contrast $\chi = 100$ and also was stationary in the grid, with the ambient medium flowing at Mach 10 from left to right. Times shown correspond to $t/t_{bc} \approx 0.2$, 1.5, and 2.5. The gray scale is logarithmic, with lightest tones about 400 times the ambient density. Eighty-five numerical zones were contained by one original clump diameter. The computation was two-dimensional on a Cartesian grid. Other computational details can be found in JKT (their model 2) and Jones & Kang (1993).

FIG. 2.—Simulated synchrotron emissivity distribution for the clump and times shown in Fig. 1. A test particle relativistic electron population was advected with the ambient medium. Its density and spectral shape were evolved according to the history of shock passages. A passive and initially uniform magnetic field was embedded in the fluid. The field was initially transverse to the flow direction. Fields in the bright features tend to follow the geometry of the features. Gray scale is logarithmic, with lightest tones about 10^4 times the bow-shock values.

ANDERSON et al. (see 421, L32)

mensurate with the growth of large amplitude R-T instabilities. A typical model behavior produced an emission e-folding timescale $\sim\frac{1}{2}t_{bc}$. Clumps with $\chi \approx 20$ and $t_{bc} \approx 40$ yr are expected to be turning on at the present epoch, predicting a brightening timescale of 20 yr, as is observed (ARI). Furthermore, radio knots in Cas A have equipartition field strengths $\sim 10^3$ times that of the average Galactic magnetic field (ARII). There are persuasive arguments for accepting these equipartition values as being indicative of the actual conditions in Cas A (Bell 1977; Anderson et al. 1991); thus, significant field amplification must have occurred beyond simple compression at shocks.

Simulations of synchrotron emission during the instability phase show structures which are very similar to those observed in very rapidly brightening radio features in Cas A. Figure 3 (Plate L8) shows a time sequence of gray-scale images of one such feature over a 12 yr interval, using data from the Cambridge 5 km telescope and the Very Large Array (VLA[1]). Note the strong similarities with the simulated knot in Figure 2 (*middle*). This Cas A feature first emerges in epoch 1982 and then brightens rapidly at a rate of $\sim 8\%$ yr^{-1}. The feature travels westward (radially inward, with respect to the shell) and develops increasingly well-pronounced trailing filamentary streamers very similar to those apparent in the simulations in Figure 2 (*middle*) and in simulated three-dimensional gaseous bullets (Stone & Norman 1992). The knot's inward-directed motion may indicate that it constitutes a subclump of material, thrown off backward when a larger clump collided with the decelerated shell (see, for example, Tenorio-Tagle & Różyczka 1984). The filamentary structure of the emissivity in Figure 2 reflects the magnetic field structure and is a consequence of the fact that amplification of the field is especially pronounced along the clump boundary where material is being stripped and dragged into the clump's wake (see Fig. 1).

A model of deceleration-induced radio brightening is also consistent with kinematic data presented in ARI, where it was demonstrated that expansion timescales of the brightest radio knots in Cas A are, on average, longer than those of fainter compact features.

Spectral index.—During the instability phase, the synchrotron spectra would be very steep if there were no preexisting cosmic rays and if there were no significant in situ acceleration by such processes as magnetic pumping or second-order Fermi acceleration. This is because most of the clump material now entrained in the amplified field regions has been processed only by weak shocks along the clump's periphery (JKT). However, if the clump travels into a medium with a large preexisting CR population (e.g., one which has been strongly processed by the passage of previous shocks), its emissivity will be dominated by background electrons entrained into the high magnetic field regions. The observed spectra will then reflect that of the background population, or the results of the bow shock, whichever is "flatter."

The latter appears to be the case in Cas A. Maps of spectral index in Cas A show that the spectra of radio emission knots are indistinguishable from those of their immediate surroundings, providing evidence for environment-based spectral regulation (ARII). Furthermore, in ARII we show that the spectral indices derived for a sample of 304 radio knots in this remnant are uncorrelated with any dynamically important quantities (e.g., knot brightness, rate of brightness change, degree of deceleration). Spectral index shows a significant correlation only with the knots' (projected) radial positions within the remnant—not with any other physical parameters (see one example in Fig. 4). In ARII, we discuss the important regulating factors for local spectral index.

Optical.—Decelerated dense clumps are no longer sources of optical emission, as the internal shock has already exited through the rear of the clump.

2.3. *The Dispersal Phase*

2.3.1. *Phenomenological Signature*

After $\sim 4t_{bc}$, the clump is completely destroyed by R-T instabilities that reduce the clump to filamentary shreds (Klein, McKee, & Colella 1990, 1994; Stone & Norman 1992). Material from the dissolved clump is dispersed and melded with the diffuse component of the ejecta.

2.3.2. *Radiative Signature*

While our simulations have not yet followed the entire clump dispersal phase, we expect synchrotron emissivity will continue to increase until the clump is torn apart by the instabilities and dispersed, or until the magnetic field strength is limited by nonlinear processes.

This picture is consistent with the distribution of radiative lifetimes measured for radio knots in Cas A. Considerably more knots are found to be brightening than fading (ARI). This suggests that most knots are cut off in their radiative prime—that in general there is no lingering fading for these compact features.

Figure 5 (Plate L8) shows an example of a clump apparently in an advanced phase of deceleration and in the process of being shredded by instabilities (compare with Figs. 1

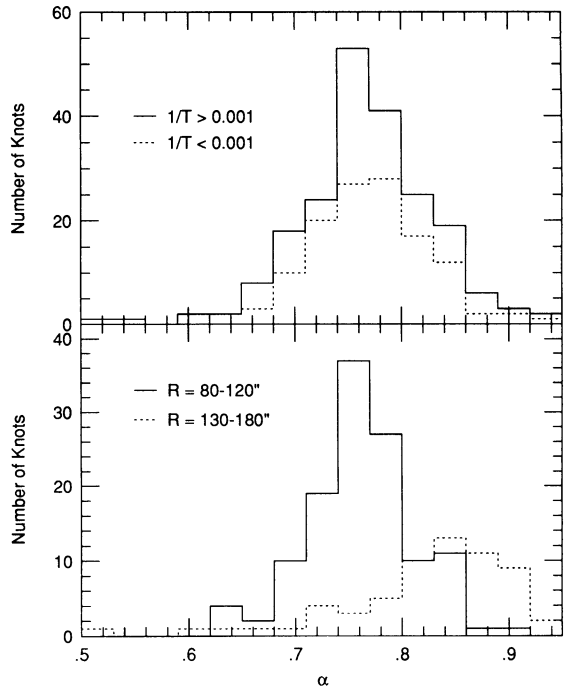

FIG. 4.—Histograms of spectral index for knot subsamples segregated by inverse expansion timescale (*above*) and radius (*below*). Annular regions of radii 80″–120″ and 130″–180″ were chosen to segregate knots within and beyond the bright radio ring.

[1] The Very Large Array is a facility of the National Radio Astronomy Observatory, operated by Associated Universities, Inc., under contract with the National Science Foundation.

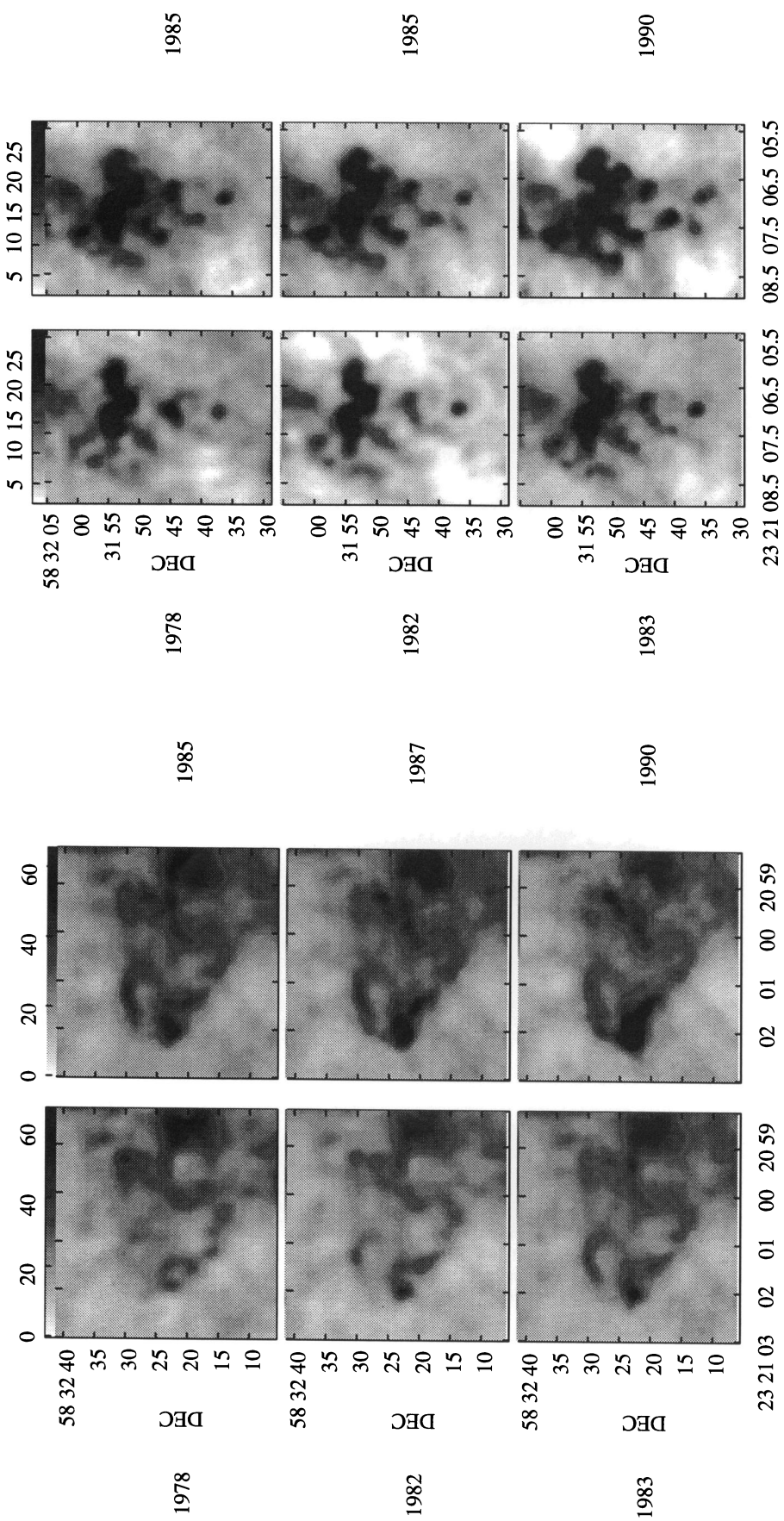

FIG. 3.—Time evolution of a radio-emitting clump in Cas A currently in the instability phase. This feature contains knots 164, 166, and 167, as tabulated in ARI.

FIG. 5.—Time evolution of a radio-emitting clump in Cas A currently in the dispersal phase. This feature contains knots 146 and 150, as tabulated in ARI; knots 53, 54, 56, and 58 brighten at later times.

[*bottom*] and 2 [*bottom*]). It is first observed as a bright V-shaped structure. Then other filaments develop, and the main V shape is degraded as blobs of material are torn from it. These secondary blobs brighten at an average rate of 6% yr^{-1}, while the original knots fade at annual rates of 9% and 3%.

3. SUMMARY OF EVOLUTIONARY MODEL

We have summarized here an evolutionary model for clumpy SNR ejecta and the associated radiative signatures. Many of the radiative and kinematic characteristics observed among emission knots in SNR Cas A show good correspondence with this model. In particular, an evolutionary sequence connecting optical-emitting knots to faint and then to bright radio knots is suggested by the models and the dynamical data presented in ARI. The degree of deceleration appears to be the major factor discriminating between these three populations of clumpy ejecta.

Observational support for this evolutionary sequence is summarized in Figure 6, where we have drawn a histogram of the inverse expansion timescales (V_R/R) measured for optical fast-moving knots (Kamper & van den Bergh 1976; van den Bergh & Kamper 1983) and for faint and bright radio knot subsets (ARI). We would propose an evolution from right to left in this plot. Additional discussion is provided in ARI.

We stress the fact that the bright radio knots in Cas A are not necessarily highlighting active particle acceleration, as has been often assumed. Rather, we would suggest that these knots demarcate sites of magnetic amplification in decelerating clumps of ejecta; active acceleration, if present, may be of secondary importance to this brightening. This interpretation is discussed further in ARII and JKT.

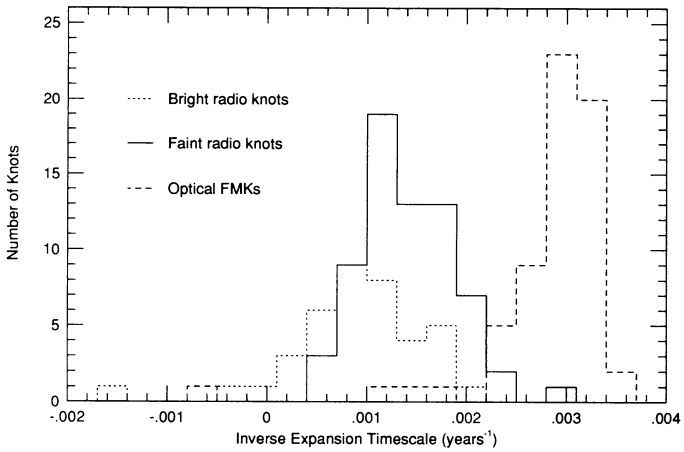

FIG. 6.—Histograms of inverse expansion timescales measured for optical FMKs (data from Kamper & van den Bergh 1976; van den Bergh & Kamper 1983), and for bright and faint radio knots (data from ARI).

The work presented here was supported at the University of Minnesota in part by the NSF through grants AST 87-20285 and AST 91-00486, by NASA through grant NAGW-2548, and by the University of Minnesota Supercomputer Institute. H. K. is supported in part by the Korea Research Foundation through the Brain Pool Program.

REFERENCES

Anderson, M. C., Keohane, J., & Rudnick, L. 1994, ApJ, submitted
Anderson, M. C., et al. 1991, ApJ, 373, 146
Anderson, M. C., & Rudnick, L. 1994a, ApJ, submitted (ARI)
———. 1994b, in preparation (ARII)
Ashworth, W. 1980, J. Hist. Astr., 11, 1
Bell, A. R. 1977, MNRAS, 179, 573
Braun, R., Gull, S. F., & Perley, R. A. 1987, Nature, 327, 395 (BGP)
Chevalier, R. A., & Klein, R. I. 1978, ApJ, 219, 994
Cowsik, R., & Sarkar, S. 1984, MNRAS, 207, 745
Dickel, J. R., & Greisen, E. W. 1979, A&A, 75, 44
Gull, S. F. 1975, MNRAS, 171, 263
Hachisu, I., Takuya, M., Nomoto, K., & Shigeyama, T. 1990, ApJ, 358, L57
Hamilton, A. J. S. 1985, ApJ, 291, 523
Jones, E. M., Smith, B. W., & Straka, W. C., 1981, ApJ, 249, 185
Jones, T. W., & Kang, H. 1993, ApJ, 402, 560
Jones, T. W., Kang, H., & Tregillis, I. L. 1993, ApJ, submitted (JKT)
Kamper, K., & van den Bergh, S. 1976, ApJS, 32, 351
Klein, R. I., McKee, C. F., & Colella, P. 1990, in Evolution of the Interstellar Medium ed. L. Blitz (ASP Conf. Ser., 127, 117
———. 1994, ApJ, 420, 213
Müller, E., & Arnett, W. D. 1982, ApJ, 261, L109
Stone, J. M., & Norman, M. L. 1992, ApJ, 390, L17
Tenorio-Tagle, G., & Różyczka, M. 1984, A&A, 137, 276
Tuffs, R. J. 1986, MNRAS, 219, 13
van den Bergh, S. 1971, ApJ, 165, 457
van den Bergh, S., & Kamper, K. W. 1983, ApJ, 268, 129